BIOCHEMISTRY
including biophysical chemistry & molecular biology

ARTICLE

pubs.acs.org/biochemistry

Structural Features and Ligand Binding Properties of Tandem WW Domains from YAP and TAZ, Nuclear Effectors of the Hippo Pathway

Claire Webb,[†] Abhishek Upadhyay,[†] Francesca Giuntini,[‡] Ian Eggleston,[‡] Makoto Furutani-Seiki,[†] Rieko Ishima,[§] and Stefan Bagby*[,†]

[†]Department of Biology and Biochemistry and [‡]Department of Pharmacy and Pharmacology, University of Bath, Claverton Down, Bath, U.K. BA2 7AY

[§]Department of Structural Biology, University of Pittsburgh School of Medicine, 3501 Fifth Avenue, Pittsburgh, Pennsylvania 15260, United States

ABSTRACT: The paralogous multifunctional adaptor proteins YAP and TAZ are the nuclear effectors of the Hippo pathway, a central mechanism of organ size control and stem cell self-renewal. WW domains, mediators of protein−protein interactions, are essential for YAP and TAZ function, enabling interactions with PPxY motifs of numerous partner proteins. YAP has single and double WW domain isoforms (YAP1 and YAP2) whereas only a single WW domain isoform of TAZ has been described to date. Here we identify the first example of a double WW domain isoform of TAZ. Using NMR, we have characterized conformational features and peptide binding of YAP and TAZ tandem WW domains (WW1−WW2). The solution structure of YAP WW2 confirms that it has a canonical three-stranded antiparallel β-sheet WW domain fold. While chemical shift-based analysis indicates that the WW domains in the tandem WW pairs retain the characteristic WW domain fold, ^{15}N relaxation data show that, within the respective WW pairs, YAP WW1 and both WW1 and WW2 of TAZ undergo conformational exchange. ^{15}N relaxation data also indicate that the linker between the WW domains is flexible in both YAP and TAZ. Within both YAP and TAZ tandem WW pairs, WW1 and WW2 bind single PPxY-containing peptide ligand concurrently and noncooperatively with sub-mM affinity. YAP and TAZ WW1−WW2 bind a dual PPxY-containing peptide with approximately 6-fold higher affinity. Our results indicate that both WW domains in YAP and TAZ are functional and capable of enhanced affinity binding to multi-PPxY partner proteins such as LATS1, ErbB4, and AMOT.

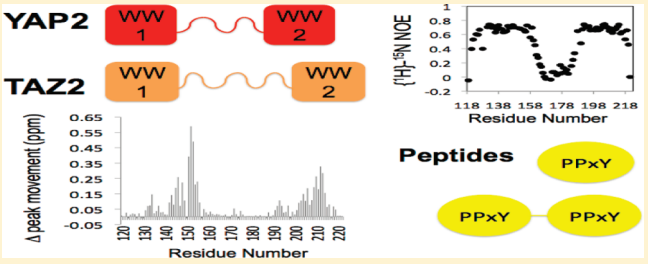

YAP, TAZ, and their *Drosophila* homologue Yorkie (Yki) are multifunctional adaptors and transcriptional regulators that can be cytoplasmic or nuclear depending on phosphorylation. Among their known roles, YAP, TAZ, and Yki are the nuclear effectors of the Hippo pathway, a core conserved signaling pathway and central mechanism of organ size regulation, spatial patterning, regulation of early embryo development, homeostasis, and regeneration following injury.[1−4] YAP and TAZ are 46% identical in amino acid sequence and have both shared and distinct regulation and function. Major components common to YAP and TAZ include an N-terminal TEAD binding region (the TEAD transcription factors are cognate DNA binding partners of YAP and TAZ), WW domain(s), and a C-terminal transcription activation domain.

The Hippo pathway was discovered in *Drosophila*.[5] In the *Drosophila* Ser/Thr kinase cassette, Hippo (Hpo), facilitated by Sav, phosphorylates itself, Sav, Mats, and Warts (Wts).[1−4] Wts phosphorylates and inhibits Yki, a potent activator of cell growth and proliferation, by 14-3-3 cytoplasmic sequestration.[6] *Drosophila* organ size is controlled via the relative cytoplasmic and nuclear levels of Yki. Hippo pathway inactivation, or Yki overexpression, causes tissue overgrowth. In vertebrates, MST1/2, SAV1, LATS1/2, and MOB1 form an analogous kinase cassette that regulates YAP and TAZ: LATS1/2 phosphorylate YAP and TAZ, causing cytoplasmic anchoring by 14-3-3. The crystal structure of a 14-3-3σ-YAP phosphopeptide complex shows 1:1 stoichiometry with mode II binding.[7] YAP phosphorylation and location correlate with cell density. Strikingly, YAP overexpression causes massive organ overgrowth with maintained organ architecture.[6,8] The role of YAP and Yki WW domains depends on cell type.[9,10]

YAP and TAZ also play key roles in the specification, self-renewal, and differentiation of stem cell lineages during development;[8,11−13] YAP and TAZ participate in maintenance of stem cell pluripotency through their interactions with TEAD[14] and Smad[12,13] transcription factors. Structural studies of the

Received: February 7, 2011
Revised: March 18, 2011
Published: March 18, 2011

YAP−TEAD interaction show that YAP N-terminal domain is natively unfolded and wraps around the immunoglobulin-like β-sandwich formed by TEAD C-terminal domain.[15−17] YAP WW domains bind the Smad1 PPxY motif,[13] whereas the TAZ coiled coil binds to Smad2/3.[12] Smad activity is dependent upon nuclear localization of Smad-YAP/TAZ complexes, which is regulated by interactions between the WW domains and PDZ binding motifs of YAP and TAZ and the Crumbs cell polarity complex in response to cell density signals.[18] YAP and TAZ have been implicated in tumorigenesis.[19−21] YAP may also have a tumor suppressive capacity. Such superficially contradictory findings probably reflect control network complexity and context dependence of YAP and TAZ function.

YAP has two major isoforms that differ in the number of WW domains: YAP1 has one WW domain, and YAP2 has two WW domains.[22,23] There are differences in expression patterns and activity of YAP isoforms, and functions of the YAP isoforms are likely to be context-dependent. Only a single WW domain isoform of TAZ has been reported to date. The WW domain is a small yet versatile protein−protein interaction module that binds proline-rich motifs or phosphoSer/Thr-Pro motifs.[24,25] The domain is named after two signature tryptophans that are 20−22 residues apart. WW domains adopt a common three-stranded antiparallel β-sheet fold. The first of the signature tryptophan residues lies on one side of the β-sheet in the hydrophobic core and is required for domain stability. On the other side of the β-sheet, the second tryptophan is located in the binding pocket. WW domains fall into five groups, I−V, based on ligand preference.[24] As group I domains, the WW domains of YAP and TAZ bind PPxY motifs in target proteins.

The Hippo pathway is rich in WW domains and their PPxY ligands: in addition to YAP, TAZ, and Yki, the Hippo pathway components Sav/SAV1 and Kibra also contain two WW domains. Dachshous, Ft1, Ft2, Ex, Hippo, Wts/LATS1/2, and the Crumbs complex components PATJ and AMOT all contain at least one PPxY motif. Tandem WW domain combinations are found in numerous other proteins and have apparently evolved particular characteristics of cooperativity/independence.[25−30] Isolated WW domains tend to be promiscuous, for example, whereas two WW domains can combine to increase specificity and/or affinity. In some cases, tandem WW domains can associate in a way that competes with ligand binding, and they can influence one another's folding or stability. In at least one example, each WW domain can bind a separate protein so that the WW pair acts as a molecular bridge. Here we demonstrate the existence of a tandem WW domain isoform of TAZ and use NMR spectroscopy to characterize conformational, dynamic, and ligand binding properties of YAP and TAZ tandem WW domains.

EXPERIMENTAL PROCEDURES

Production of TAZ cDNA Plasmids. RNA was isolated from two adult Hd-rR medaka fish and used to synthesize a cDNA library with the TaKaRa PCR kit. Nested PCR was used to amplify TAZ cDNA: the product of PCR with forward and reverse primers TGGAGATTTGCTTCGACTCTG and GCCTATAGCCAGGTGAGCAG was used as template for a second PCR with forward primer GACTCTGACTTCTGGCGACAT and the same reverse primer. The DNA fragments were purified, phosphorylated with polynucleotide kinase, and ligated into pBluescript SK-. The resulting plasmids were transformed into Mach1 *E. coli* for selection of successful clones. The DNA was then sequenced (GATC Biotech).

Cloning, Expression, and Purification of Recombinant WW Domain Fragments. DNA sequences encoding YAP and TAZ single and tandem WW domain fragments were amplified by PCR using medaka full length YAP and TAZ cDNA in pBluescript SK- as template and cloned into pBG101 (Vanderbilt University Structural Biology Center). Residue numbers are as follows: 119−162, 182−222, 119−222 for YAP WW1, WW2, and WW1−WW2 and 103−147, 177−218, 103-218 for TAZ WW1, WW2 and WW1−WW2. *E. coli* BL21-(DE3) were grown at 37 °C to OD_{600} 0.6−0.9, induced and cultured for 3 h. Following cell harvest, lysis, and 60000*g* centrifugation, WW domains were purified by metal ion chromatography. The 6His-GST tag was removed with 3C protease followed by a second HisTrap stage and then anion exchange.

Peptide Synthesis. Single PPxY peptide GTPPPPYTVG was assembled on an Activo P11 automated peptide synthesizer (Activotec) on a 0.12 mmol scale, on preloaded Fmoc-Gly Wang resin (Novabiochem), according to 9-fluorenylmethoxycarbonyl (Fmoc) solid phase protocols. The peptide was characterized by high resolution mass spectrometry (Bruker MicroTOF). Dual PPxY peptide GTPPPPYTVGGGGGGGTPPPPYTVG was bought from Thermo Fisher Scientific.

Sample Preparation, NMR Spectroscopy, and Data Analysis for Tandem WW Domains. ^{15}N YAP WW1−WW2 was exchanged into 50 mM potassium phosphate pH 5.5, 100 mM NaCl, 0.5 mM EDTA, and ^{15}N TAZ WW1−WW2 was exchanged into 20 mM Tris pH 7.5, 100 mM NaCl. NMR sample concentrations were determined by UV absorption and SDS-PAGE. YAP WW1−WW2 NMR data were acquired at 18 °C and TAZ WW1−WW2 NMR data at 27.5 °C. Solution conditions and data acquisition temperature were selected on the basis of protein solubility and ^{1}H−^{15}N HSQC quality. Backbone assignments were obtained from double and triple resonance data using CCPN Analysis;[31] since some of the expected WW1 peaks were not observed in YAP and TAZ WW1−WW2 triple resonance spectra, backbone assignments of YAP and TAZ WW1 domain alone were needed to complete YAP and TAZ WW1−WW2 backbone assignment.

In order to monitor WW−peptide binding, YAP and TAZ tandem WW ^{1}H−^{15}N HSQC spectra were recorded as a function of increasing peptide concentration. The average chemical shift change of each NH peak was calculated using $\Delta\delta_{av}$ (ppm) = $[(\Delta\delta^2\mathrm{HN} + \Delta\delta^2\mathrm{N}/25)/2]^{1/2}$. The affinity of each WW domain within WW1−WW2 for single PPxY peptide was calculated using chemical shift movement of binding site residues. Dissociation constants, K_d, were determined by minimizing a target function, $\chi^2 = \Sigma(\Delta\delta_{av}{}^{exp} - \Delta\delta_{av}{}^{cal})^2/(\Delta_{err})^2$. Here, $\Delta\delta_{av}{}^{exp}$ and $\Delta\delta_{av}{}^{cal}$ indicate experimental and calculated chemical shift changes, and Δ_{err} indicates experimental error (estimated 0.005 ppm against normalized $\Delta\delta_{av}$ ppm). In each minimization, two parameters (K_d and the relative saturated chemical shift) were optimized using Matlab 2009 (Mathworks Inc.). In addition, the $\Delta\delta_{av}{}^{cal}$ values in the determination of K_d for single PPxY peptide binding to WW1 or WW2 were calculated using eqs 17−19 in ref 32. Similarly, $\Delta\delta_{av}{}^{cal}$ values for dual PPxY peptide binding to WW1−WW2 were calculated using eqs 14−16 in ref 32, assuming 1:1 binding without allosteric effects (see Results).

Heteronuclear NMR experiments to determine ^{15}N longitudinal relaxation rate (R_1), ^{15}N transverse relaxation rate (R_2), and $\{^{1}\mathrm{H}\}$-^{15}N NOE parameters for YAP and TAZ tandem WW

Figure 1. Sequence alignment of human and medaka YAP and TAZ WW domains. Alignments were made using ClustalW[55] and the panel generated with Boxshade. The β-strand locations are from YAP WW1[39] and YAP WW2 (this work) structures. Initial residue numbers are indicated.

domains were recorded on a Bruker Avance 600 spectrometer with cryo-probe. R_1 and R_2 spectra were recorded at seven relaxation time points: 0, 0.05, 0.1, 0.2, 0.3, 0.5, and 0.8 s for R_1 and 0, 8, 16, 32, 48, 64, and 80 ms for R_2. NOE values were determined using ^{15}N peak intensity recorded with and without 3 s ^{1}H saturation. In addition, ^{15}N CPMG relaxation dispersion was recorded for YAP WW1−WW2 at a constant time of 40 ms with effective field strength ν_{CP} ($1/4t_{cp}$) of 50, 100, 200, 400, 500, and 700 Hz to verify the regions that undergo conformational exchange.[33] Spectra were processed using NMRPipe/NMRDraw,[34] and relaxation data were analyzed using in-house software.[35]

Sample Preparation, NMR Spectroscopy, and Structure Calculation of YAP WW2. Purified YAP WW2 was exchanged into 50 mM potassium phosphate pH 5.5, 200 mM NaCl, 5 mM EDTA, and NMR data acquired at 30 °C. NMR data were processed as described above[34] and analyzed using CCPN analysis.[31] Structures were calculated and assessed as previously described.[36]

RESULTS

Identification of Tandem WW Domain Isoform of TAZ. YAP is known to have single and double WW domain isoforms (YAP1 and YAP2),[22,23] whereas only a single WW domain isoform of TAZ has been described. We sequenced several medaka TAZ cDNA plasmids prior to use as template for PCR amplification of WW domain fragments. Two splice forms of medaka TAZ were identified: the previously known single WW domain isoform (TAZ1) and a novel isoform (TAZ2) with a second WW domain separated from the first WW domain by 45 residues, such that the TAZ2 inter-WW domain linker is 10 residues longer than the YAP2 linker (Figure 1). The tandem WW domains of medaka YAP2 and TAZ2 are overall 59% identical and 70% similar in sequence. The individual WW domains show higher homology than the tandem constructs: YAP and TAZ WW1 domains are 82% identical and the WW2 domains 78% identical, so the inter-WW linkers differ more between YAP2 and TAZ2 than the WW domains. Medaka and human YAP WW1 domains are 100% identical, the WW2 domains are 89% identical and 96% similar, and tandem domains are 78% identical and 88% similar. Medaka and human TAZ WW1 domains are 70% identical and 78% similar. Given this high sequence conservation, there is a high probability that conclusions from this study will apply to YAP and TAZ WW domains from a wide range of vertebrates.

Conformational Features of YAP and TAZ Tandem WW Domains. The chemical shift dispersion of backbone NH peaks in

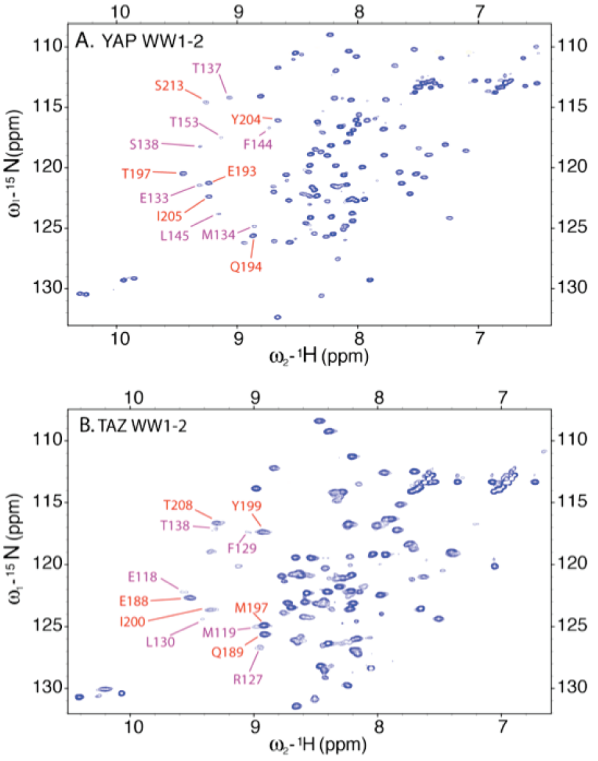

Figure 2. YAP and TAZ tandem WW domain ^{1}H−^{15}N HSQC spectra. Labels indicate peaks around ^{1}H chemical shift 9 ppm that are weaker in WW1 than peaks from equivalent residues in WW2 (purple labels correspond to WW1 and red to WW2 peaks within WW1−WW2).

^{1}H−^{15}N HSQC spectra of YAP and TAZ WW1−WW2 indicates that WW2 is folded and that at least a substantial fraction of WW1 domains in the WW1−WW2 population is folded. For both YAP and TAZ WW1−WW2, the WW1 peaks around proton chemical shift values of 9 ppm in ^{1}H−^{15}N-HSQC spectra are weaker than the equivalent WW2 peaks (Figure 2): in YAP, the weak WW1 peaks and their WW2 equiv are E133 (WW1) and E193 (WW2), M134 and Q194, T137 and T197, F144 and Y204, L145 and I205; and in TAZ, E118 (WW1) and E188 (WW2), M119 and Q189, R127 and M197, F129 and Y199, L130 and I200. As described below, signal broadening arises from a chemical exchange contribution to transverse relaxation rates. The corresponding absence of certain peaks from YAP and TAZ WW1−WW2 triple resonance data meant that NMR data from isolated WW1 domains (with relatively weak but detectable peaks) were required to assign

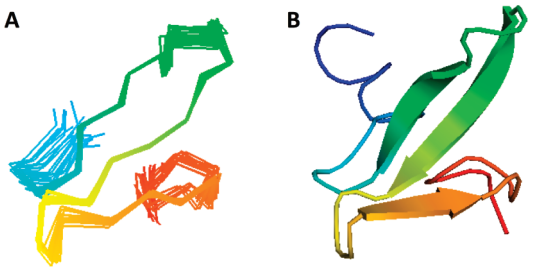

Figure 3. Solution structure of YAP WW2. (A) Superimposition and (B) average structure of the 20 lowest energy structures from 100 calculations colored from blue at the N-terminus to orange at the C-terminus (PDB code 2L4J). The figure was generated using Pymol.

Table 1. Structural Statistics Summary for the 20 Lowest Energy Structures of YAP WW2

total number of NOE restraints	358
intraresidue	108
sequential and medium range ($i+1$ to $i+4$)	113
long range	137
number of dihedral angle restraints	46
number of hydrogen bond restraints	20
mean rmsd of backbone atoms[a]	0.34 Å
mean rmsd of non-hydrogen atoms[a]	1.04 Å
average number of NOE violations	1.8
average number of dihedral angle violations	0
Ramachandran plot regions (% residues)[b]	
most favored	81.8
additionally allowed	18.2
generously allowed	0
disallowed	0

[a] Rmsd from mean structure calculated over residues 190−197, 201−207, and 210−214. [b] Residues 190−214.

several WW1 residues within WW1−WW2. Relative to YAP WW1−WW2 $^{1}H-^{15}N$ HSQC, the TAZ WW1−WW2 $^{1}H-^{15}N$ HSQC exhibits more heterogeneous signal patterns; five Trp indole NH signals are observed in the indole region around ^{1}H chemical shift 10 ppm for TAZ WW1−WW2, for example, rather than the four expected, indicating that at least one Trp indole NH undergoes chemical exchange.

Solution Structure of YAP WW2 and Chemical Shift-Based Secondary Structure Analysis of YAP WW1 and TAZ WW1 and WW2. Since the YAP WW2 structure has remained undetermined, and in order to verify that YAP WW2 adopts a typical WW fold, we determined the solution structure of YAP WW2. The final structures (Figure 3 and Table 1) were obtained using NOE-derived distance restraints, hydrogen bond restraints, and Φ and Ψ dihedral angle TALOS+ restraints.[37] YAP WW2 indeed has a characteristic WW fold; it comprises three antiparallel β-strands (residues 192−197, 201−207, 210−214), connected by two short flexible loops, which form a twisted β-sheet. A cluster of hydrophobic side chains lies on the opposite face of the β-sheet to the ligand binding site and the regions N- and C-terminal to the WW domain core curve around this hydrophobic region.

Comparison of YAP WW2 and WW1−WW2 using chemical shift-based secondary structure prediction indicates that WW2 retains this three-stranded β-sheet structure in the tandem WW domain pair. Detailed structural analysis was not undertaken for YAP and TAZ

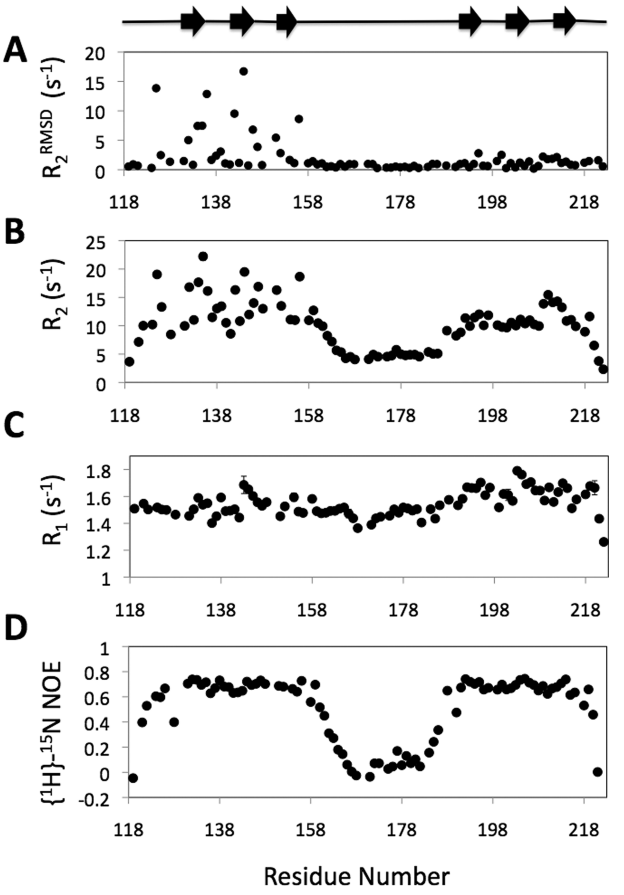

Figure 4. Backbone dynamics of YAP WW1−WW2. (A) R_2 dispersion, (B) ^{15}N R_2, (C) ^{15}N R_1, and (D) {^{1}H}−^{15}N NOE values as a function of residue number. The β-strand locations are from YAP WW1[39] and YAP WW2 (this work) structures.

tandem WW domains because, as mentioned above, numerous YAP and TAZ WW1 signals are weak and TAZ WW1−WW2 peak intensities are heterogeneous (Figure 2). Sequence homology (Figure 1) and chemical shift-based secondary structure prediction, however, indicate that TAZ WW1 and WW2 adopt a typical WW domain fold. Analysis of ^{1}H, ^{13}C, and ^{15}N chemical shift values indicates there are β-strands at residues W132−K136, R142−N146, and T152−W154 in isolated YAP WW1; W132−K136, R142−N146, and T152−W154 in WW1 within YAP WW1−WW2; W117−K121, R127−N131, and T137−L140 in isolated TAZ WW1; the first and third β-strands in WW1 within TAZ WW1−WW2 could not be verified due to incomplete Cα and Cβ assignments, but the second β-strand location matches that in isolated TAZ WW1; and E188−V191, M197−D201, and T207−V210 in WW2 within TAZ WW1−WW2. The predicted YAP WW1 β-strand locations agree closely with those observed in YAP WW1−peptide structures.[38,39]

Dynamic Instability of the Tandem WW Domains. We acquired ^{15}N relaxation data to identify the cause of heterogeneous $^{1}H-^{15}N$ HSQC signal intensities in YAP and TAZ WW1−WW2 spectra. The WW1 domain of YAP WW1−WW2 exhibited R_2 rmsd in the R_2 dispersion data and high CPMG R_2 values (Figure 4A,B), indicating that there is significant conformational exchange in YAP WW1. The YAP WW1 residues that undergo significant conformational exchange within WW1−WW2 include D125, W132, M134, A135, K136, R142,

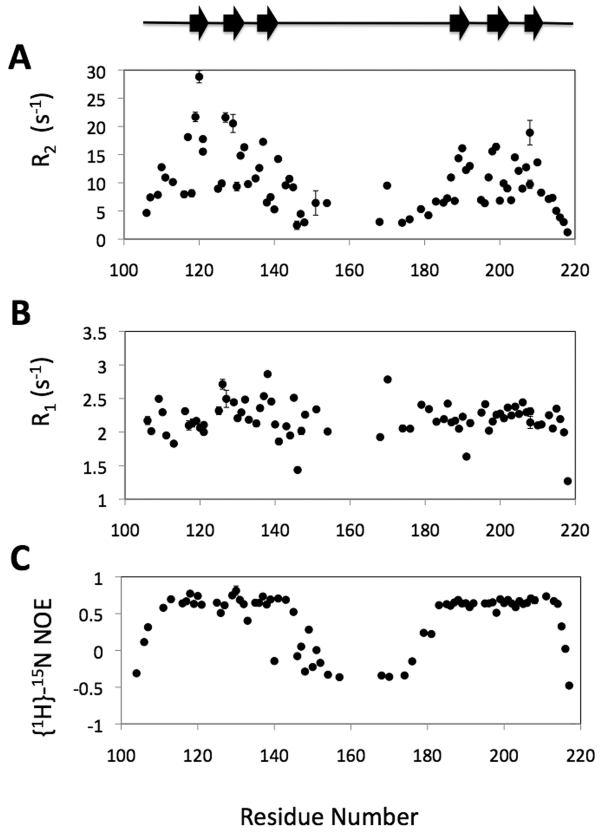

Figure 5. Backbone dynamics of TAZ WW1−WW2. (A) ^{15}N R_2, (B) ^{15}N R_1, and (C) {^{1}H}−^{15}N NOE values as a function of residue number. Secondary structure elements were predicted from chemical shift values using TALOS+[37] (WW1 values were taken from data for isolated WW1 domain rather than tandem WW1−WW2). Several residues in the TAZ linker could not be assigned.

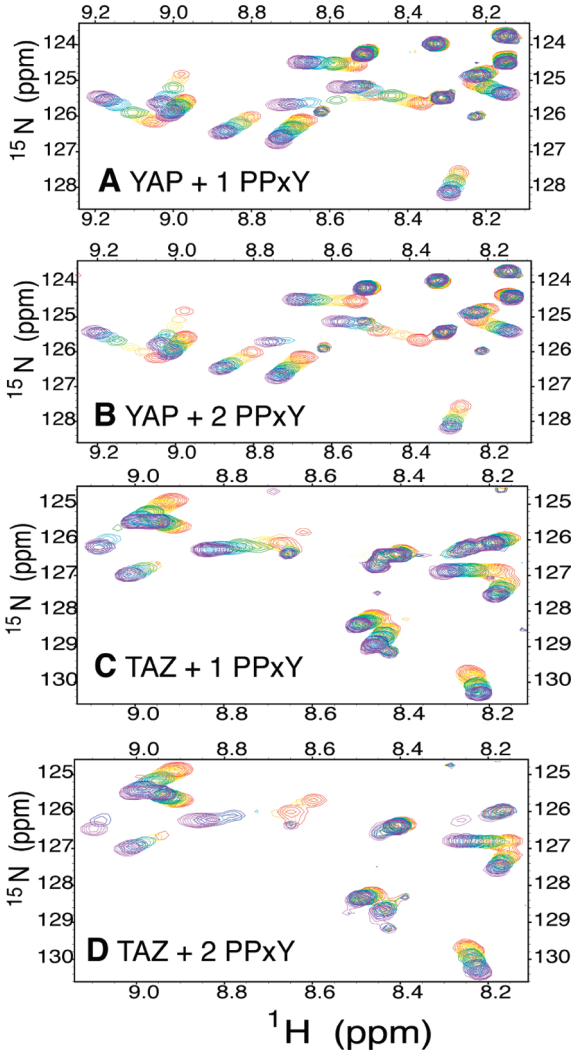

Figure 6. WW−PPxY peptide titration ^{1}H−^{15}N HSQC spectra. Sections of overlaid spectra for YAP and TAZ tandem WW domains with (A, C) single and (B, D) dual PPxY peptides (start and end points are in red and purple).

F144, T151, and D156. The side chains of these residues are on the opposite side of the β-sheet to the peptide binding site. These observations are consistent with the weak WW1 signal intensities observed in the YAP WW1−WW2 ^{1}H−^{15}N HSQC spectrum (Figure 2).

TAZ WW1−WW2 exhibited elevated ^{15}N R_2 values in both WW domains (Figure 5), consistent with the observed heterogeneous, and overall weaker, signal intensities in the TAZ WW1−WW2 HSQC spectrum. These elevated R_2 values are not due to rapid amide−water proton exchange at pH 7.5 in the antiphase $N_{X,Y}H_Z$ term generated during the CPMG period but due to chemical exchange, because a qualitative $R_{1\rho}$ experiment with relatively short delays (0−32 ms) at $B_1/2\pi$ = 2 kHz also showed elevated $R_{1\rho}$ values in the two WW domains (data not shown).

In spite of the similar molecular masses of YAP and TAZ tandem WW pair constructs, the smallest R_2 in the β-sheet region (assumed to experience the smallest chemical exchange effect) is ~8 s^{-1} in TAZ WW1−WW2, slightly smaller than that of YAP WW1−WW2 (~10 s^{-1}). The average R_1 in TAZ WW1−WW2 is larger (2.2 ± 0.25 s^{-1}) than that of YAP WW1−WW2 (1.5 ± 0.10 s^{-1}). These differences in R_1 and R_2 indicate that overall molecular motion is greater in TAZ WW1−WW2 than in YAP WW1−WW2. On the basis of the Stokes−Einstein equation for a single molecular rotation and water viscosity,[40] the difference in experimental temperatures for YAP (18 °C) and TAZ (27.5 °C) is predicted to result in a 15% change in rotational correlation times. Although the difference in R_2 between YAP and TAZ WW1−WW2 is within a range that can be explained simply by the temperature difference, the difference in R_1 may not be so explained (see below). This suggests that additional dynamics occur in TAZ WW1−WW2 such as domain motions, equilibrium between folded and unfolded forms, or weak dimerization.

The Linker between WW1 and WW2 Is Unstructured. Backbone NH peaks of YAP and TAZ WW1−WW2 linker residues are mostly within the central region of ^{1}H−^{15}N HSQC spectra around ^{1}H chemical shift 8 ppm, consistent with a lack of structure in the linker. {^{1}H}−^{15}N NOE values, moreover, average 0.064 for YAP linker residues 166−184 and −0.207 for TAZ linker residues 148−176 (Figures 4D and 5C), indicating significant mobility of NH bond vectors on the picosecond to nanosecond time scale. This compares with average {^{1}H}−^{15}N NOE values of 0.664 and 0.672 for YAP WW1 (residues 122−159) and WW2 (residues 190−219) and 0.635 and 0.646 for TAZ WW1 (residues 111−143) and WW2 (residues 183−213), indicating that the WW

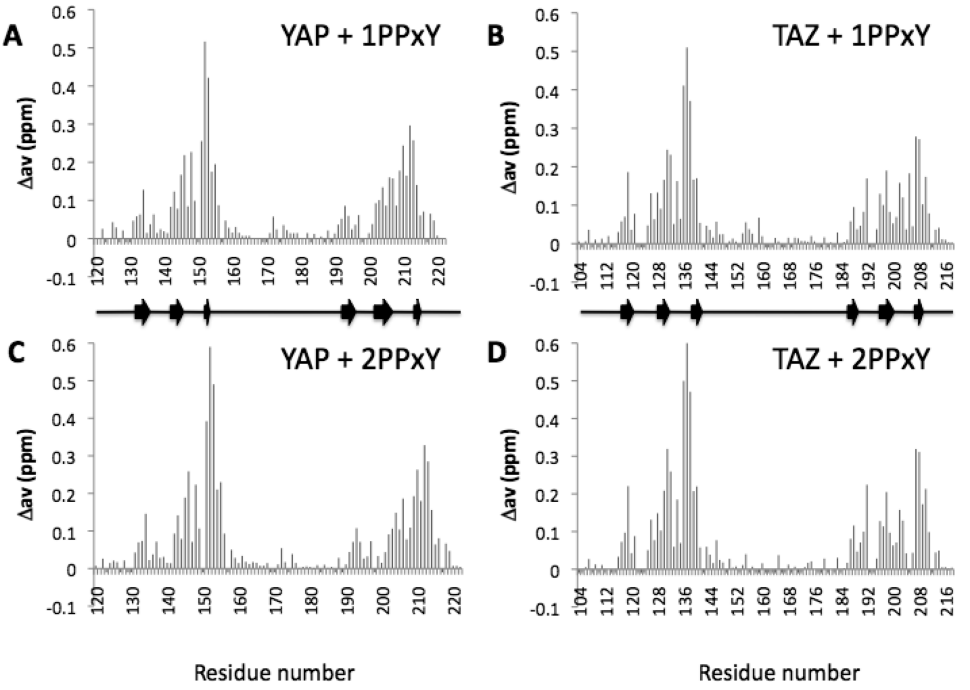

Figure 7. Chemical shift changes upon tandem WW domain−peptide interaction. Average chemical shift movement of each assigned peak after the final addition of single PPxY peptide (top) and dual PPxY peptide (bottom) to (A, C) YAP and (B, D) TAZ WW1−WW2. Unassigned and proline residues are shown as small negative values. TAZ secondary structure elements were predicted from chemical shift values using TALOS+.[37]

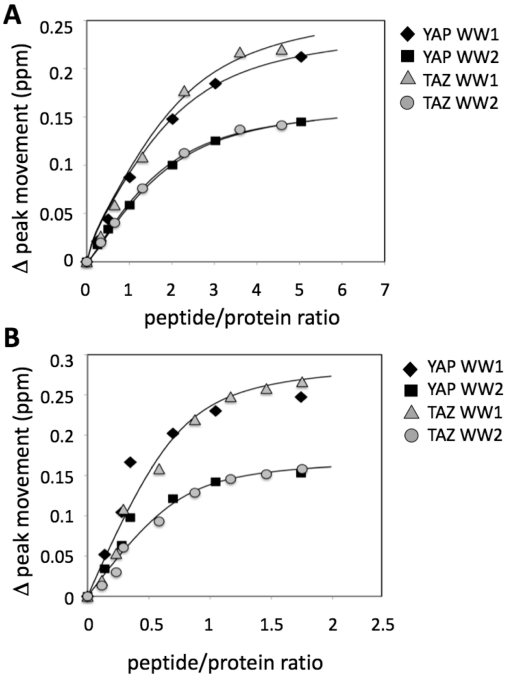

Figure 8. Average chemical shift movement of binding site residues upon peptide binding. YAP and TAZ WW1 and WW2 within WW1−WW2 binding to (A) single and (B) dual PPxY peptides.

domains within WW1−WW2 are relatively rigid. In addition, we did not observe any medium range NOEs within the YAP and TAZ linkers in ^{15}N-edited 3D NOESY spectra. There is thus strong evidence that the inter-WW domain linker region in both YAP2 and TAZ2 is unstructured and highly flexible. It is therefore possible that there is interdomain mobility; such mobility would significantly affect R_1, consistent for example with the fact that the difference in R_1 between YAP and TAZ WW1−WW2 is not explained simply by difference in temperature of data acquisition. In both YAP and TAZ WW1−WW2, since there are large R_2 values, probably due to conformational exchange, rotational correlation times and subsequent estimation of relative domain orientations are not obtainable from ^{15}N relaxation data.

Interaction of YAP and TAZ Tandem WW Domains with PPxY Peptides. In order to assess WW1−WW2 binding to ligand, the single PPxY-containing peptide GTPPPPYTVG that has been used in previous studies of YAP WW1 structure and binding[39] or tandem PPxY-containing peptide GTPPPPYTV-GGGGGGGTPPPPYTVG was titrated into an NMR sample of ^{15}N-labeled YAP or TAZ WW1−WW2. Binding was monitored via ^{1}H−^{15}N HSQC spectra recorded at each titration point (Figure 6). Both WW domains within YAP and TAZ WW1−WW2 interacted with GTPPPPYTVG and with GTPPPP-YTVGGGGGGGTPPPPYTVG (Figure 7).

We used the average chemical shift movement of residues known to form the peptide binding site, at each addition of peptide, to calculate dissociation constant values for YAP and TAZ WW1−WW2. The affinities for GTPPPPYTVG of WW1 and WW2 within WW1−WW2 are similar for YAP and TAZ, with YAP K_d values of 284 ± 52 μM (WW1) and 281 ± 55 μM (WW2) and TAZ K_d values of 330 ± 116 μM (WW1) and 273 ± 116 μM (WW2). This similarity of dissociation constant values between WW1 and WW2 is consistent with the high sequence homology between the domains (52% identity between YAP2 WW1 and WW2 and 59% identity between TAZ2 WW1 and WW2).

The dual PPxY peptide interacted with tandem WW domains of YAP and TAZ with higher affinity than single PPxY peptide, as evidenced by significant chemical shift changes at lower peptide: protein ratio for the dual PPxY peptide (Figure 8). WW1 and WW2 showed almost identical titration curve shapes, indicating

concomitant, nondomain-selective binding (see Discussion). The K_d for TAZ WW1-WW2 binding to dual PPxY peptide was 48.5 ± 12 μM. The K_d of YAP WW1−WW2 for dual PPxY peptide was calculated to be similar to TAZ WW1−WW2, but the calculation had a low confidence level with $\chi^2/n > 8$. The pattern of chemical shift changes upon dual PPxY peptide interaction was very similar to that upon single PPxY peptide binding (Figure 7). This indicates that the interaction mode of each WW domain is the same with single and dual PPxY peptides. Larger chemical shift changes in the second and third β-strands are consistent with the expected prominent ligand binding role of residues within these strands such as Y143, L145, and W154 (YAP WW1) and Y203, I205, and W214 (YAP WW2). The corresponding residues in human YAP are Y188, L190, and W199 in WW1 and Y247, I249, and W258 in WW2.

Linker residue chemical shifts changed to a much lesser extent than the WW domain peaks (Figure 7). Consistent with these small chemical shift changes, average linker $\{^1H\}-^{15}N$ NOE values of 0.038 and −0.18 for YAP and TAZ WW1−WW2 bound to dual PPxY peptide were similar to those of the unbound YAP and TAZ WW1−WW2 of 0.064 and −0.207.

DISCUSSION

Identification of TAZ Double WW Domain Isoform. The discovery of YAP1 was reported in 1994 followed by the tandem WW domain isoform YAP2 in 1995.[22,23] We have found no mention of a tandem WW domain isoform of TAZ from any species in the literature or databases (Ensembl and Genbank). Our identification in medaka of a tandem WW isoform of TAZ, TAZ2, could therefore represent the first example of tandem WW TAZ. It is possible that TAZ2 will be found in other organisms. There has been limited analysis of the biological function of the two major YAP isoforms, YAP1 and YAP2. YAP2, for example, was shown to be a stronger coactivator of transcription than YAP1, and an attempt was made to compare their tissue expression patterns in mouse, but the YAP1 transcript could not be detected. Subsequent reports suggest that functions of the YAP isoforms are likely to be context-dependent.

YAP WW2 Adopts a Typical WW Fold and YAP WW1 and TAZ WW1 and WW2 Undergo Conformational Exchange. The structure of YAP WW1 has only been studied in complex with PPxY-containing peptide.[38,39] We have determined the structure of unliganded YAP WW2. Comparison of the YAP WW2 structure with other WW domain structures, including various YAP WW1−peptide structures, revealed rmsd values around 1.5 Å. The one noticeably variable region among the structures is the loop that connects β-strands 1 and 2, previously identified as a specificity enhancing loop.[41] Sequence homology and chemical shift-based secondary structure prediction indicate that TAZ WW domains also adopt a typical WW domain fold.

The conformational exchange of YAP WW1 within YAP WW1−WW2 (Figure 4) is consistent with the weaker WW1 peaks in $^1H-^{15}N$ HSQC spectra of YAP WW1−WW2 (Figure 2). These YAP WW1 signals remain weak even in the isolated WW1 domain, suggesting that broadening of YAP WW1 signals within WW1−WW2 is not primarily due to interaction with WW2. As YAP WW2 does not undergo significant conformational exchange on the μs−ms time scale (Figure 4), we considered sequence differences that may help to explain the difference in conformational homogeneity between YAP WW1 and WW2. Examples include charged residues (K136 and R142) in WW1 compared to hydrophobic residues (I196 and I202) in the corresponding locations of WW2 (Figure 1). These residues are located at the C-terminal end of the first β-strand and N-terminal end of the second β-strand; their side chains are adjacent and protrude into the environment of hydrophobic core residues W154/W214 and F144/Y204 (WW1/WW2). Interestingly, a previous molecular simulation study found that YAP WW1 was significantly less stable than FBP28 WW domain.[42] Within TAZ WW1−WW2, both WW1 and WW2 undergo conformational exchange. In TAZ WW1, K121 and R127 correspond to YAP WW1 residues K136 and R142. TAZ WW2 contains V191 and M197 in positions corresponding to YAP residues I196 and I202, indicating that more subtle sequence differences between YAP WW2 and TAZ WW2 in additional positions contribute to conformational exchange in TAZ WW2. The solution conditions and temperature of NMR data acquisition selected for the WW1−WW2 constructs, based on $^1H-^{15}N$ HSQC quality and protein solubility, included different temperatures and pH values and near-physiological salt concentrations, so we surmise that the observed conformational exchange is not condition specific and is likely to persist in physiological conditions.

Flexibility of the Inter-WW Domain Linker. Previous studies on tandem WW domains have revealed both a rigid, 10-residue α-helical linker (Prp40[27]) and flexible linkers with no secondary structural elements (Su(dx),[43] FBP21,[30] Smurf2[28]). The rigid Prp40 linker restricts the two WW domains to a defined relative orientation whereas the inter-WW domain linker regions of Su(dx), FBP21, and Smurf2 consist of a flexible loop spanning 20, 12, and 20 residues, respectively, with some restriction to inter-WW domain motion. The inter-WW linkers of YAP and TAZ, at 35 and 45 residues, respectively, are significantly longer. Chemical shift and backbone $\{^1H\}-^{15}N$ NOE data (Figures 2, 4, and 5) indicate that the region linking the WW domains in YAP and TAZ is unstructured and highly flexible, so the YAP and TAZ inter-WW domain linkers resemble the Su(dx), FBP21, and Smurf2 linkers more than the Prp40 linker.

Interactions of YAP and TAZ WW1−WW2 with PPxY-Containing Ligands. During the tandem WW−PPxY peptide NMR titrations, chemical shift changes occurred for peaks from both WW domains of YAP and TAZ with each addition of peptide, suggesting that the WW domains interact concurrently with peptide. $^1H-^{15}N$ chemical shift changes indicate that each WW domain within YAP and TAZ WW1−WW2 has essentially equal affinity for the single PPxY motif. The K_d values obtained for the single PPxY peptide interaction (in the range 273 ± 116 to 330 ± 116 μM) are similar to those measured previously for Su(dx) WW3−WW4 binding to a Notch PPxY peptide ligand[26] but significantly higher than the K_d value of 1.7 ± 0.4 μM for Smurf WW2−WW3 binding to a Smad PPxY peptide. In the Smurf−Smad case, Smurf WW2 augments and enhances Smurf−Smad WW−peptide interaction relative to WW3 alone.[28] Relative to these group I WW domains, the tandem group III WW domains of FBP21 show weaker binding to group III PPR motif peptides (K_d values in the range 1−3 mM).[30]

TAZ WW1−WW2 binds the dual PPxY peptide with higher affinity (48.5 ± 12 μM) than single PPxY peptide. On the basis of the chemical shift changes, YAP WW1−WW2 affinity for the dual PPxY peptide was estimated to be similar to that of TAZ WW1−WW2. The 6-fold enhancement of YAP and TAZ WW1−WW2 affinity for dual PPxY peptide over single PPxY peptide is smaller than the >10-fold affinity enhancement observed

Table 2. Binding Partners of YAP and TAZ WW Domains

protein	binding partner	number of PPxY
LATS1	YAP[44] and TAZ[45]	2
LATS2	YAP[44] and TAZ[45]	1
p73	YAP[46]	2[a]
PRGP2	YAP[47]	1
ErbB4	YAP[48]	3 or 2
Smad1	YAP[13]	1
Runx2	YAP[49] and TAZ[50]	1
PEBP2	YAP[51]	1
ASPP2	YAP[52] and TAZ[53]	1
AMOT	YAP and TAZ[18]	2
DVL2	TAZ[54]	1

[a] YAP preferentially binds the second PY motif.

for FBP21 WW1−WW2 binding to peptide with two proline-rich motifs over peptide with one proline-rich motif.[30] Inter-WW domain cooperativity is unlikely to account for enhanced affinity of YAP and TAZ WW1−WW2 for the dual PPxY peptide since chemical shift changes occurred concurrently for WW1 and WW2, in a similar manner to the single PPxY titrations. Unlike the FBP21 case, moreover, dual PPxY peptide binding exerted little effect on linker residue backbone NH chemical shifts (Figure 7) and, consistent with this, little effect on $\{^1H\}-^{15}N$ NOE values; this indicates that the linker remains largely unstructured and flexible. This particular dual PPxY peptide therefore does not induce allosteric conformational change in YAP and TAZ WW1−WW2. The data are more consistent with an avidity-based mechanism for enhanced affinity in which binding of a PPxY motif to one WW domain brings the other PPxY motif into proximity to the other WW domain, limiting the spatial search required for execution of the second WW−PPxY binding event. On the basis of the small effects on linker residues and the lower K_d of dual PPxY binding, it is possible that the two domain-bound form interconverts between one domain-bound forms. We do not exclude the possibility that dual PPxY peptides with different inter-PPxY linkers would induce allosteric conformational change in YAP and TAZ WW1−WW2.

Although the mechanism is not completely clear, enhanced dual PPxY binding by tandem YAP and TAZ WW domains has been clearly established in this study. Such enhanced affinity of dual PPxY binding may be important in YAP2 or TAZ2 interaction with binding partners such as LATS1, ErbB4, and AMOT that contain multiple PPxY motifs (Table 2). The two PPxY motifs in LATS1, a kinase that is part of the core Hippo pathway cassette and that phosphorylates YAP and TAZ, are separated by about 180 amino acids, but it is possible that these PPxY motifs are spatially close enough to bind to tandem WW domains in a single molecule of YAP2 or TAZ2. Immunoprecipitation experiments, for example, suggest that both LATS1 PPxY motifs and both YAP WWs are necessary for full strength YAP−LATS1 binding. In the case of ErbB4, in which two of the PPxY motifs are 17 amino acids apart, YAP2 coactivates ErbB4-regulated genes more strongly than YAP1.

CONCLUSIONS

We have discovered the first example of a double WW domain isoform of TAZ. The structure of YAP WW2, 78% identical to TAZ WW2, was demonstrated to be similar to other WW domains. Within WW1−WW2, WW1, and WW2 affinities for PPxY ligand are almost identical. YAP and TAZ WW1−WW2 bind single PPxY peptide with affinity in the range 270−330 μM and dual PPxY peptide with ∼50 μM affinity. The linker between the WW domains is highly flexible and essentially unaffected during interactions with single and dual PPxY peptides. The inter-WW linker is 10 residues longer in TAZ than in YAP; this could contribute to ligand affinity differences and may provide a mechanism to tune the selectivity of YAP and TAZ for partner proteins, for example, those with multiple PPxY motifs such as LATS1, ErbB4, and AMOT.

AUTHOR INFORMATION

Corresponding Author

*E-mail: bsssb@bath.ac.uk. Phone: +441225 386436. Fax: +441225 386779.

Funding Sources

This work was supported by a BBSRC doctoral training grant (to C.W.) and US National Science Foundation research grant MCB 0814905 (to R.I.).

ABBREVIATIONS

Fmoc, 9-fluorenylmethoxycarbonyl; Hpo, Hippo; HSQC, heteronuclear single quantum coherence; NMR, nuclear magnetic resonance; NOE, nuclear Overhauser effect; PCR, polymerase chain reaction; rmsd, root-mean-square deviation; Sav, Salvador; SDS PAGE, sodium dodecyl sulfate polyacrylamide gel electrophoresis; TAZ, transcriptional coactivator with PDZ binding motif; UV, ultraviolet; Wts, Warts; YAP, Yes associated protein.

REFERENCES

(1) Zhao, B., Li, W., Lei, Q., and Guan, K. L. (2010) The Hippo-YAP pathway in organ size control and tumorigenesis: an updated version. *Genes Dev. 24*, 862–874.

(2) Oh, H., and Irvine, K. D. (2010) Yorkie: the final destination of Hippo signaling. *Trends Cell Biol. 20*, 410–417.

(3) Sudol, M., and Harvey, K. F. (2010) Modularity in the Hippo signalling pathway. *Trends Biochem. Sci. 35*, 627–633.

(4) Pan, D. J. (2010) The Hippo signaling pathway in development and cancer. *Dev. Cell 19*, 491–505.

(5) Tapon, N., Harvey, K. F., Bell, D. W., Wahrer, D. C. R., Schiripo, T. A., Haber, D. A., and Hariharan, I. K. (2002) *salvador* promotes both cell cycle exit and apoptosis in *Drosophila* and is mutated in human cancer cell lines. *Cell 35*, 467–478.

(6) Dong, J. X., Feldmann, G., Huang, J. B., Wu, S., Zhang, N. L., Comerford, S. A., Gayyed, M. F., Anders, R. A., Maitra, A., and Pan, D. J. (2007) Elucidation of a universal size-control mechanism in *Drosophila* and mammals. *Cell 130*, 1120–1133.

(7) Schumacher, B., Skwarczynska, M., Rose, R., and Ottmann, C. (2010) Structure of a 14-3-3σ-YAP phosphopeptide complex at 1.15 Å resolution. *Acta Crystallogr. F 66*, 978–984.

(8) Camargo, F. D., Gokhale, S., Johnnidis, J. B., Fu, D., Bell, G. W., Jaenisch, R., and Brummelkamp, T. R. (2007) YAP1 increases organ size and expands undifferentiated progenitor cells. *Curr. Biol. 17*, 2054–2060.

(9) Zhao, B., Kim, J., Ye, X., Lai, Z. C., and Guan, K. L. (2009) Both TEAD-binding and WW domains are required for the growth stimulation and oncogenic transformation activity of Yes-associated protein. *Cancer Res. 69*, 1089–1098.

(10) Zhang, X. M., Milton, C. C., Humbert, P. O., and Harvey, K. F. (2009) Transcriptional output of the Salvador/Warts/Hippo pathway is controlled in distinct fashions in *Drosophila melanogaster* and mammalian cell lines. *Cancer Res. 69*, 6033–6041.

(11) Cao, X. W., Pfaff, S. L., and Gage, F. H. (2008) YAP regulates neural progenitor cell number via the TEA domain transcription factor. *Genes Dev. 22*, 3320–3334.

(12) Varelas, X., Sakuma, R., Samavarchi-Tehrani, P., Peerani, R., Rao, B. M., Dembowy, J., Yaffe, M. B., Zandstra, P. W., and Wrana, J. L. (2008) TAZ controls Smad nucleocytoplasmic shuttling and regulates human embryonic stem-cell self-renewal. *Nat. Cell Biol. 10*, 837–848.

(13) Alarcon, C., Zaromytidou, A. I., Xi, Q. R., Gao, S., Yu, J. Z., Fujisawa, S., Barlas, A., Miller, A. N., Manova-Todorova, K., Macias, M. J., Sapkota, G., Pan, D. J., and Massague, J. (2009) Nuclear CDKs drive Smad transcriptional activation and turnover in BMP and TGF-β pathways. *Cell 139*, 757–769.

(14) Lian, I., Kim, J., Okazawa, H., Zhao, J. G., Zhao, B., Yu, J. D., Chinnaiyan, A., Israel, M. A., Goldstein, L. S. B., Abujarour, R., Ding, S., and Guan, K. L. (2010) The role of YAP transcription coactivator in regulating stem cell self-renewal and differentiation. *Genes Dev. 24*, 1106–1118.

(15) Chen, L. M., Chan, S. W., Zhang, X. Q., Walsh, M., Lim, C. J., Hong, W. J., and Song, H. W. (2010) Structural basis of YAP recognition by TEAD4 in the Hippo pathway. *Genes Dev. 24*, 290–300.

(16) Li, Z., Zhao, B., Wang, P., Chen, F., Dong, Z. H., Yang, H. R., Guan, K. L., and Xu, Y. H. (2010) Structural insights into the YAP and TEAD complex. *Genes Dev. 24*, 235–240.

(17) Tian, W., Yu, J. Z., Tomchick, D. R., Pan, D. J., and Luo, X. L. (2010) Structural and functional analysis of the YAP-binding domain of human TEAD2. *Proc. Natl. Acad. Sci. U.S.A. 107*, 7293–7298.

(18) Varelas, X., Samavarchi-Tehrani, P., Narimatsu, M., Weiss, A., Cockburn, K., Larsen, B. G., Rossant, J., and Wrana, J. L. (2010) The Crumbs complex couples cell density sensing to Hippo-dependent control of the TGF-β-SMAD pathway. *Dev. Cell 19*, 831–844.

(19) Overholtzer, M., Zhang, J., Smolen, G. A., Muir, B., Li, W., Sgroi, D. C., Deng, C. X., Brugge, J. S., and Haber, D. A. (2006) Transforming properties of YAP, a candidate oncogene on the chromosome 11q22 amplicon. *Proc. Natl. Acad. Sci. U.S.A. 103*, 12405–12410.

(20) Zender, L., Spector, M. S., Xue, W., Flemming, P., Cordon-Cardo, C., Silke, J., Fan, S. T., Luk, J. M., Wigler, M., Hannon, G. J., Mu, D., Lucito, R., Powers, S., and Lowe, S. W. (2006) Identification and validation of oncogenes in liver cancer using an integrative oncogenomic approach. *Cell 125*, 1253–1267.

(21) Chan, S. W., Lim, C. J., Guo, K., Ng, C. P., Lee, I., Hunziker, W., Zeng, Q., and Hong, W. J. (2008) A role for TAZ in migration, invasion, and tumorigenesis of breast cancer cells. *Cancer Res. 68*, 2592–2598.

(22) Sudol, M. (1994) Yes-associated protein (Yap65) is a proline-rich phosphoprotein that binds to the SH3 domain of the Yes proto-oncogene product. *Oncogene 9*, 2145–2152.

(23) Sudol, M., Bork, P., Einbond, A., Kastury, K., Druck, T., Negrini, M., Huebner, K., and Lehman, D. (1995) Characterization of the mammalian Yap (Yes-associated protein) gene and its role in defining a novel protein module, the WW domain. *J. Biol. Chem. 270*, 14733–14741.

(24) Ball, L. J., Kuhne, R., Schneider-Mergener, J., and Oschkinat, H. (2005) Recognition of proline-rich motifs by protein-protein-interaction domains. *Angew. Chem., Int. Ed. 44*, 2852–2869.

(25) Sudol, M., Recinos, C. C., Abraczinskas, J., Humbert, J., and Farooq, A. (2005) WW or WoW: The WW domains in a union of bliss. *IUBMB Life 57*, 773–778.

(26) Jennings, M. D., Blankley, R. T., Baron, M., Golovanov, A. P., and Avis, J. M. (2007) Specificity and autoregulation of Notch binding by tandem WW domains in Suppressor of Deltex. *J. Biol. Chem. 282*, 29032–29042.

(27) Wiesner, S., Stier, G., Sattler, M., and Macias, M. J. (2002) Solution structure and ligand recognition of the WW domain pair of the yeast splicing factor Prp40. *J. Mol. Biol. 324*, 807–822.

(28) Chong, P. A., Lin, H., Wrana, J. L., and Forman-Kay, J. D. (2010) Coupling of tandem Smad ubiquitination regulatory factor (Smurf) WW domains modulates target specificity. *Proc. Natl. Acad. Sci. U.S.A. 107*, 18404–18409.

(29) Ramirez-Espain, X., Ruiz, L., Martin-Malpartida, P., Oschkinat, H., and Macias, M. J. (2007) Structural characterization of a new binding motif and a novel binding mode in group 2 WW domains. *J. Mol. Biol. 373*, 1255–1268.

(30) Huang, X. J., Beullens, M., Zhang, J. H., Zhou, Y., Nicolaescu, E., Lesage, B., Hu, Q., Wu, J. H., Bollen, M., and Shi, Y. Y. (2009) Structure and function of the two tandem WW domains of the pre-mRNA splicing factor FBP21 (Formin-binding protein 21). *J. Biol. Chem. 284*, 25375–25387.

(31) Vranken, W. F., Boucher, W., Stevens, T. J., Fogh, R. H., Pajon, A., Llinas, P., Ulrich, E. L., Markley, J. L., Ionides, J., and Laue, E. D. (2005) The CCPN data model for NMR spectroscopy: Development of a software pipeline. *Proteins: Struct. Funct. Bioinf. 59*, 687–696.

(32) Fielding, L. (2007) NMR methods for the determination of protein-ligand dissociation constants. *Prog. Nucl. Magn. Reson. Spectrosc. 51*, 219–242.

(33) Tollinger, M., Skrynnikov, N. R., Mulder, F. A. A., Forman-Kay, J. D., and Kay, L. E. (2001) Slow dynamics in folded and unfolded states of an SH3 domain. *J. Am. Chem. Soc. 123*, 11341–11352.

(34) Delaglio, F., Grzesiek, S., Vuister, G. W., Zhu, G., Pfeifer, J., and Bax, A. (1995) NMRPipe: a multidimensional spectral processing system based on UNIX pipes. *J. Biomol. NMR 6*, 277–293.

(35) Freedberg, D. I., Ishima, R., Jacob, J., Wang, Y. X., Kustanovich, I., Louis, J. M., and Torchia, D. A. (2002) Rapid structural fluctuations of the free HIV protease flaps in solution: relationship to crystal structures and comparison with predictions of dynamics calculations. *Protein Sci. 11*, 221–232.

(36) Upadhyay, A., Burman, J. D., Clark, E. A., Leung, E., Isenman, D. E., van den Elsen, J. M. H., and Bagby, S. (2008) Structure-function analysis of the C3 binding region of *Staphylococcus aureus* immune subversion protein Sbi. *J. Biol. Chem. 283*, 22113–22120.

(37) Shen, Y., Delaglio, F., Cornilescu, G., and Bax, A. (2009) TALOS+: a hybrid method for predicting protein backbone torsion angles from NMR chemical shifts. *J. Biomol. NMR 44*, 213–223.

(38) Pires, J. R., Taha-Nejad, F., Toepert, F., Ast, T., Hoffmuller, U., Schneider-Mergener, J., Kuhne, R., Macias, M. J., and Oschkinat, L. (2001) Solution structures of the YAP65 WW domain and the variant L30K in complex with the peptides GTPPPPYTVG, N-(n-octyl)-GPPPY and PLPPY and the application of peptide libraries reveal a minimal binding epitope. *J. Mol. Biol. 314*, 1147–1156.

(39) Macias, M. J., Hyvonen, M., Baraldi, E., Schultz, J., Sudol, M., Saraste, M., and Oschkinat, H. (1996) Structure of the WW domain of a kinase-associated protein complexed with a proline-rich peptide. *Nature 382*, 646–649.

(40) Cho, C. H., Urquidi, J., Singh, S., and Robinson, G. W. (1999) Thermal offset viscosities of liquid H_2O, D_2O, and T_2O. *J. Phys. Chem. B 103*, 1991–1994.

(41) Verdecia, M. A., Bowman, M. E., Lu, K. P., Hunter, T., and Noel, J. P. (2000) Structural basis for phosphoserine-proline recognition by group IV WW domains. *Nat. Struct. Biol. 7*, 639–643.

(42) Ibragimova, G. T., and Wade, R. C. (1999) Stability of the β-sheet of the WW domain: A molecular dynamics simulation study. *Biophys. J. 77*, 2191–2198.

(43) Fedoroff, O. Y., Townson, S. A., Golovanov, A. P., Baron, M., and Avis, J. M. (2004) The structure and dynamics of tandem WW domains in a negative regulator of Notch signaling, Suppressor of Deltex. *J. Biol. Chem. 279*, 34991–35000.

(44) Zhang, J., Smolen, G. A., and Haber, D. A. (2008) Negative regulation of YAP by LATS1 underscores evolutionary conservation of the *Drosophila* Hippo pathway. *Cancer Res. 68*, 2789–2794.

(45) Lei, Q. Y., Zhang, H., Zhao, B., Zha, Z. Y., Bai, F., Pei, X. H., Zhao, S., Xiong, Y., and Guan, K. L. (2008) TAZ promotes cell proliferation and epithelial-mesenchymal transition and is inhibited by the Hippo pathway. *Mol. Cell. Biol. 28*, 2426–2436.

(46) Strano, S., Munarriz, E., Rossi, M., Castagnoli, L., Shaul, Y., Sacchi, A., Oren, M., Sudol, M., Cesareni, G., and Blandino, G. (2001) Physical interaction with Yes-associated protein enhances p73 transcriptional activity. *J. Biol. Chem. 276*, 15164–15173.

(47) Kulman, J. D., Harris, J. E., Xie, L., and Davie, E. W. (2007) Proline-rich Gla protein 2 is a cell-surface vitamin K-dependent protein

that binds to the transcriptional coactivator Yes-associated protein. *Proc. Natl. Acad. Sci. U.S.A. 104*, 8767–8772.

(48) Komuro, A., Nagai, M., Navin, N. E., and Sudol, M. (2003) WW domain-containing protein YAP associates with ErbB-4 and acts as a co-transcriptional activator for the carboxyl-terminal fragment of ErbB-4 that translocates to the nucleus. *J. Biol. Chem. 278*, 33334–33341.

(49) Zaidi, S. K., Sullivan, A. J., Medina, R., Ito, Y., van Wijnen, A. J., Stein, J. L., Lian, J. B., and Stein, G. S. (2004) Tyrosine phosphorylation controls Runx2-mediated subnuclear targeting of YAP to repress transcription. *EMBO J. 23*, 790–799.

(50) Hong, J. H., Hwang, E. S., McManus, M. T., Amsterdam, A., Tian, Y., Kalmukova, R., Mueller, E., Benjamin, T., Spiegelman, B. M., Sharp, P. A., Hopkins, N., and Yaffe, M. B. (2005) TAZ, a transcriptional modulator of mesenchymal stem cell differentiation. *Science 309*, 1074–1078.

(51) Yagi, R., Chen, L. F., Shigesada, K., Murakami, Y., and Ito, Y. (1999) A WW domain-containing Yes-associated protein (YAP) is a novel transcriptional co-activator. *EMBO J. 18*, 2551–2562.

(52) Espanel, X., and Sudol, M. (2001) Yes-associated protein and p53-binding protein-2 interact through their WW and SH3 domains. *J. Biol. Chem. 276*, 14514–14523.

(53) Liu, C. Y., Lv, X., Li, T., Xu, Y., Zhou, X., Zhao, S., Xiong, Y., Lei, Q. Y., and Guan, K. L. (2011) PP1 Cooperates with ASPP2 to dephosphorylate and activate TAZ. *J. Biol. Chem. 286*, 5558–5566.

(54) Varelas, X., Miller, B. W., Sopko, R., Song, S. Y., Gregorieff, A., Fellouse, F. A., Sakuma, R., Pawson, T., Hunziker, W., McNeill, H., Wrana, J. L., and Attisano, L. (2010) The Hippo pathway regulates Wnt/β-Catenin signaling. *Dev. Cell 18*, 579–591.

(55) Thompson, J. D., Higgins, D. G., and Gibson, T. J. (1994) CLUSTAL W: improving the sensitivity of progressive multiple sequence alignment through sequence weighting, position-specific gap penalties and weight matrix choice. *Nucleic Acids Res. 22*, 4673–4680.